JOURNAL OF GEOPHYSICAL RESEARCH, VOL. 94, NO. D6, PAGES 8497–8509, JUNE 20, 1989

Least Independent Variables Method for Simulation of Tropospheric Ozone

D. J. JACOB, S. SILLMAN,[1] J. A. LOGAN, AND S. C. WOFSY

Division of Applied Sciences and Department of Earth and Planetary Sciences
Harvard University, Cambridge, Massachusetts

We describe a method for simulating photochemical production of O_3 in a continental-scale tropospheric model with only six independent chemical variables representing tracers transported in the model. The tracers are two primary hydrocarbon families, CO, NO_x, peroxyacylnitrates, and odd oxygen (O_x). A chemical module is developed to compute the production and loss rates of tracers over a model time step of 4 hours, using only information on the tracer concentrations input to the module at the beginning of the time step. Test simulations for summertime conditions at mid-latitudes indicate little loss in accuracy compared to detailed model simulations of chemistry with high time resolution. Minimization of the number of tracers and use of a long time step reduces computer time and storage requirements. In addition, parameterization of the chemical computation is facilitated, allowing further sayings in computer time.

1. INTRODUCTION

Large-scale simulations of tropospheric O_3 are presently limited by the computational requirements of photochemical models. Photochemical production of O_3 from NO_x and hydrocarbons is significant on both regional and global scales [*Levy et al.*, 1985; *Logan*, 1985; *Logan and Kirchhoff*, 1986; *Liu et al.*, 1987; *Trainer et al.*, 1987]. Proper representation of this source requires a three-dimensional chemical tracer model (CTM) that can resolve the complex distributions of NO_x and hydrocarbons and can account for the non-linear dependence of O_3 production on the concentrations of these species. The task is complicated by the large number of species that participate in O_3 production and by the intricacy of their chemistry. Detailed photochemical mechanisms include over 100 atmospheric species [*Lurmann et al.*, 1986], and the associated chemical lifetimes range from a few milliseconds to many days. Our objective in this paper is to show that O_3 production can be computed accurately in a continental-scale CTM with only 6 chemical tracers, using a time step of 4 hours. We refer to the method involved as the "least independent variables" (LIV) method. Combination of the LIV method with a parameterization of the chemical computation [*Dunker*, 1986; *Marsden et al.*, 1987] realizes considerable savings in computer time and storage, making it feasible to conduct CTM simulations on seasonal time scales.

Development of the LIV method is part of an effort by our research group to design a CTM for climatological studies of tropospheric O_3, with a focus on summertime episodes over North America. The CTM uses the grid and the meteorology of the Goddard Institute for Space Studies (GISS) general circulation model [*Hansen et al.*, 1983; *Prather et al.*, 1987]; the model domain extends over the entire North American continent in order to avoid influences from boundary conditions. The resolution is coarse, 4° in latitude by 5° in longitude, with seven layers in the vertical extending to the tropopause (the lowest 3 layers extend to approximately 500, 1200, and 2600 m above ground level), and a time step of 4 hours. Subgrid spatial resolution is provided by conservation of first- and second-order moments in tracer concentration [*Prather*, 1986]. The CTM simulates fairly well the distribution of ^{222}Rn (lifetime 5.5 days) over North America, indicating that boundary layer convection is reasonably represented (D. J. Jacob and M. J.Prather, Radon-222 as a test of convection in a general circulation model, submitted to *Tellus*, 1989). For photochemical applications, small-scale highly polluted environments such as cities and power plants are treated with a nested subgrid scheme, the Plumes Model, which resolves the non-linear dependence of photochemistry on the concentrations of NO_x and hydrocarbons, (S. Sillman et al., A regional-scale model for photochemical production of ozone in the United States that includes the effects of urban and power plant plumes, submitted to *Journal of Geophysical Research*, 1989; hereinafter Sillman et al. (1989)).

The chemical module of the CTM must compute the chemical production and loss of tracers over a model time step, using as information only the tracer concentrations at the beginning of that time step. This computation is done with the specially designed LIV module, which we describe in this paper. For application to the CTM, the production minus loss rates of tracers computed with the LIV module will be fitted to parameterized polynomial functions of independent chemical and meteorological variables, where the independent chemical variables are the tracer concentrations (C. M. Spivakovsky et al. Tropospheric OH and seasonal variations of atmospheric halocarbons: separating the influences of chemistry and transport, submitted to *Journal of Geophysical Research*, 1989; hereinafter Spivakovsky et al. (1989)). Construction of the parameterized functions requires an exhaustive number of LIV module calculations sampling the n-dimensional space defined by the independent variables. As the number of independent variables increases, efficient sampling of the space becomes disproportionately more difficult. The LIV method is designed to facilitate the parameterization procedure by minimizing the number of tracers, and hence the number of independent chemical variables. Combination of the LIV method with parameterization of the chemical module decreases computer time by 3 orders of magnitude over that required by standard kinetic solvers (Spivakovsky et al., 1989).

[1] Now at Department of Atmospheric, Oceanic, and Space Sciences, University of Michigan, Ann Arbor.

Paper number 89JD00308.
0148-0227/89/89JD-00308$05.00

TABLE 1. Independent Chemical Variables of the LIV Method

Independent Variable	Composition[a]
HC1	Propane 13%, C_{4-5} alkanes 32%, C_{6-8} alkanes 20%, C_{4-5} alkylnitrates 2%, C_{6-8} alkylnitrates 6%, benzene 8%, toluene 12%,ethylene 7%
HC2	Isoprene 100% (daytime non-urban below 800 mb); Isoprene 30%, propene 70% (all other conditions)
CO	
NO_x	$NO + NO_2 + NO_3 + (2x)N_2O_5 + HNO_2 + HNO_4$
PANs	PAN 70%, other peroxyacylnitrates 30%
O_x	$O_3 + O + NO_2 + HNO_4 + (2x)NO_3 + (3x)N_2O_5$

[a] Proportions for HC1 and HC2 are in ppbC units.

Our approach in the LIV method is to group atmospheric species with similar properties into "lumped" tracers, and to make extensive use of steady-state assumptions for secondary species. The 6 tracers are selected on the basis of the detailed photochemical mechanism of *Lurmann et al.* [1986], but the procedure should be adaptable readily to any photochemical mechanism. The accuracy of the LIV method will be evaluated in this paper by comparison with detailed photochemical model simulations in which all atmospheric species are treated as independent chemical variables and conserved from time step to time step.

The paper is organized as follows. In section 2 we discuss the selection of chemical tracers and the lumping procedure. The chemical module is described in section 3. Extension of the chemical module to concentrated source regions is presented in section 4. The accuracy of the overall approach is evaluated in section 5. Concluding remarks are in section 6.

2. SELECTION OF CHEMICAL TRACERS

Under given meteorological conditions, the O_3 production rate in an air parcel is determined mainly by the concentrations of hydrocarbons, CO, and reactive nitrogen species. In the LIV method we lump O_3, primary hydrocarbons, and reactive nitrogen species into 5 chemical tracers (Table 1). Carbon monoxide is simulated as a separate tracer. We discuss in this section the choice of tracers, in the context of the detailed photochemical mechanism of *Lurmann et al.* [1986]. This mechanism has been shown to simulate observations for a wide range of environments, including smog chamber experiments [*Lurmann et al.*, 1986], the St. Louis urban airshed [*Sillman*, 1987], and the Amazon forest [*Jacob and Wofsy*, 1988]. The latter study introduced some modifications necessary to extend the mechanism to sub-ppb levels of NO_x.

The detailed mechanism of *Lurmann et al.* [1986] includes a full suite of hydrocarbon reactions to describe the photochemical production of O_3. Table 2 lists the individual hydrocarbons participating in the mechanism, and their mean chemical lifetimes (day and night) over North America in summer. We segregate the hydrocarbons into 4 classes as shown in Table 2. Class I and class II hydrocarbons are simulated as two separate tracers, HC1 and HC2, with units of ppbC (ppb of carbon atoms). Class III hydrocarbons are assumed to be at steady state between chemical production and loss. Class IV hydrocarbons are assumed to be present at fixed concentrations. We justify these different treatments below.

Class I groups photochemically important primary hydrocarbons with lifetimes in excess of a day. Alkylnitrates are included in this class because they have lifetimes of a few days and are similar to alkanes in terms of O_3 production potential [*Lurmann et al.*, 1986]. The main sink for class I hydrocarbons is reaction with OH to form peroxy radicals, RO_2. The RO_2 radicals may react with NO, producing O_3, or with HO_2, consuming odd hydrogen. Carbonyls produced from the RO_2 + NO reactions may react further to produce or consume O_3. Two arguments can be made

TABLE 2. Chemical Lifetimes of Hydrocarbons

Species	Sinks	Lifetime, hours: day	night
	Class I		
Propane	OH	57	>[a]
C_{4-5}-alkanes	OH, NO_3	27	>
C_{6-8}-alkanes	OH, NO_3	12	>
C_{4-5}-alkylnitrates	OH	69	>
C_{6-8}-alkylnitrates	OH	17	>
Benzene	OH	58	>
Toluene	OH	11	>
Ethylene	OH, O_3	8.5	>
	Class II		
Isoprene	OH, O_3, NO_3	0.8	1.1
Propene	OH, O_3, NO_3	2.5	83
Butene	OH, O_3, NO_3	0.5	1.7
Xylene	OH	2.9	>
	Class III		
Formaldehyde	OH, NO_3, hv	3.0	>
Acetaldehyde	OH, NO_3, hv	4.1	250
C_{3-5}-aldehydes	OH, NO_3, hv	3.2	250
Methylethylketone	OH, NO_3, hv	44	>
Phenol	OH, NO_3	2.5	0.2
Cresols	OH, NO_3	1.6	0.03
Dimethylphenol	OH, NO_3	1.0	0.02
Unsaturated dicarbonyls	OH, hv	1.1	>
Aromatic aldehydes	OH, hv	2.0	>
Methylvinylketone	OH, O_3, NO_3	3.9	5.8
Methacrolein	OH, O_3, NO_3	2.2	35
Hydroxyacetaldehyde	OH, NO_3, hv	4.4	660
Methylglyoxal	OH, hv	1.3	>
Glyoxal	OH, hv	2.6	>
Glycolaldehyde	OH, hv	3.9	>
	Class IV		
Ethane	OH	255	>
Acetone	OH, hv	140	>
Methanol	OH	69	>
Ethanol	OH	20	>
Formic acid	OH	215	>
Acetic acid	OH	117	>
Methyl hydroperoxide	OH, hv	6.1	>
Organic peroxides	OH, hv	6.4	>

Chemical lifetimes (gas-phase reactions only) are calculated from the *Lurmann et al.* [1986] mechanism with T= 298 K, O_3 = 50 ppb, OH = 4×10^6 molecules cm^{-3} (day), NO_3=8×10^8 molecules cm^{-3} (night). Photolysis rates are calculated for clear summer skies (latitude 40° , solar declination 20°, surface albedo 0.1) at 1000 mbar and 1400 LT.

[a] Longer than 1000 hours.

TABLE 3. Ozone and Odd Hydrogen Yields From the Atmospheric Decomposition of Primary Hydrocarbons

	Ozone		Odd Hydrogen	
Species	Moles per Mole	Moles per Mole C	Moles per Mole	Moles per Mole C
		Class I		
Propane	4.1	1.4	0.17	0.06
$C_{4,5}$ alkanes	6.6	1.5	0.48	0.11
$C_{6,8}$ alkanes	9.2	1.3	0.54	0.08
Benzene	7.2	1.2	0.35	0.06
Toluene	10.2	1.4	1.85	0.26
Ethylene	3.7	1.9	0.70	0.35
		Class II		
Isoprene	6.8	1.4	1.80	0.36
Propene	6.7	2.2	0.92	0.31
Butene	5.3	1.3	1.45	0.37
Xylene	13.9	1.7	4.04	0.51

Odd hydrogen is defined as the sum of OH and peroxy radicals. The yields are defined as the number of O_3 or odd hydrogen molecules produced from the decomposition of one hydrocarbon molecule, and are derived from the detailed photochemical mechanism of *Lurmann et al.* [1986] with the following assumptions: (1) peroxy radicals are removed by reaction with NO (i.e., PANs are at steady state and NO is in large excess of HO_2); (2) secondary hydrocarbons with chemical lifetimes less than 12 hours are decomposed further by reaction with OH or photolysis. The branching ratios for decomposition of secondary hydrocarbons are computed assuming OH = 4×10^6 molecules cm^{-3} and photolysis rates for clear summer skies (latitude 40°, solar declination 20°, surface albedo 0.1) at 925 mbar and 1400 LT.

for lumping class I hydrocarbons into one single tracer. First, class I hydrocarbons have comparable lifetimes (one to a few days), and they produce O_3 and odd hydrogen with roughly similar yields per carbon atom (Table 3). Second, measurements at rural sites in the eastern United States suggest that class I hydrocarbons are present in relatively constant proportions [*Arnts and Meeks*, 1981; *Sexton and Westberg*, 1984; W. Lonnemann, personal communication, 1988]. We average all measurements available from the 3 above references to derive a typical mix of class I hydrocarbons, which defines the reactivity of the HC1 tracer (Table 1). In the case of alkylnitrates no measurements are available, and the proportions are based on photochemical model calculations for typical rural conditions [*Sillman*, 1987].

Class II groups primary hydrocarbons with average chemical lifetimes of a few hours in the daytime. These hydrocarbons tend to produce O_3 mainly in the vicinity of their sources, in contrast to class I hydrocarbons. Therefore they cannot be included as part of HC1. In addition, class II hydrocarbons are significantly stronger sources of odd hydrogen than class I hydrocarbons (Table 3). Class II hydrocarbons produce O_3 and odd hydrogen with similar yields per carbon atom, so we lump them into one chemical tracer, HC2. Measurements of class II hydrocarbons in rural regions are scarce, particularly in the case of isoprene [*Altshuller*, 1983]. We expect that isoprene should be the dominant contributor to HC2 in the boundary layer over North America during summer days, because isoprene emission fluxes from vegetation [*Lamb et al.*, 1987] are larger than the combined emission fluxes of propene, butene, and xylene [*Environmental Protection Agency (EPA)*, 1986]. Therefore we assume that HC2 has the reactivity of isoprene in the lower troposphere (1000 - 800 mbar) during the day. At higher altitudes, over cities, and at night, propene and xylene are likely to be major contributors to HC2. Under these conditions we assume that HC2 has the reactivity of a 70:30 mixture of propene and isoprene.

The chemical lifetime of isoprene is generally shorter than 4 hours, which could argue for a steady state treatment in the lowest CTM layer based on a balance between emission and chemical loss. The advantage of this approach would be to avoid transporting isoprene as a tracer. However the steady-state assumption is inadequate in low-NOx environments, where the chemical lifetime of isoprene is much higher than the mean value given in Table 2 [*Jacob and Wofsy*, 1988]. Significant vertical transport of isoprene can occur in these environments; measurements over the Amazon forest indicate isoprene concentrations in excess of 1 ppb at 760 m altitude both in the day and at night [*Rasmussen and Khalil*, 1988]. Considering the importance of isoprene as a source of odd hydrogen in rural and remote atmospheres [*Trainer et al.*, 1987; *Sillman*, 1987], we must allow for its transport above the lowest CTM layer.

Carbon monoxide is transported as a tracer independent of HC1 or HC2, for two reasons. First, oxidation of CO does not produce odd hydrogen. Second, the lifetime of CO is several weeks, so that CO contributes little to O_3 production in regions where nonmethane hydrocarbons are abundant [*Liu et al.*, 1987], but it can be the principal contributor to O_3 production in the remote troposphere [*Chameides and Walker*, 1973; *Fishman et al.*, 1979]. Another important O_3 precursor in the remote troposphere is CH_4, but the relative variability of the CH_4 concentration about its mean value (1.7 ppm) is sufficiently small that the mean value can be assumed in the chemical computation.

The hydrocarbons in class III arise mainly from the atmospheric degradation of class I and class II hydrocarbons. Most have chemical lifetimes of a few hours in the daytime. They can be broken down into several chemical families: aldehydes, ketones, dicarbonyls, phenols, and cresols. Each of these families contributes in a different manner to the photochemical production of O_3, and in principle each should be transported as one or more separate tracers. An economical alternative, which we adopt here, is to assume that the concentrations of class III hydrocarbons are at steady state between chemical production and loss. With this assumption, the class III hydrocarbons do not constitute independent chemical variables, and they need not be included as tracers in the CTM. At night the lifetimes of class III hydrocarbons are long (except for phenols and cresols), and sources are negligible; therefore we assume steady state with an assumed air parcel composition for the previous afternoon. Nighttime concentrations of phenols and cresols are fixed at low values because removal by NO_3 is fast (Table 2). Clearly, the steady state treatment for class III hydrocarbons is not rigorous. We assume however that departures from steady state are sufficiently small that they should not affect significantly the rate of O_3 production. Large departures from steady state could occur when photochemical activity is low, but O_3 production is slow in any case under such conditions. Errors in the nighttime concentrations should not be critical because class III hydrocarbons play little role in nighttime chemistry.

The remaining hydrocarbons (class IV) have long lifetimes, and contribute little to O_3 production; we assume that they are present at fixed concentrations, 2 ppb for ethane and 1 ppb for each of the other species in Table 2. Organic peroxides could possibly play a significant role in the odd hydrogen budget [*Kleinman*, 1986], but kinetic data regarding their chemical sources and sinks are largely unavailable. Washout and in-cloud reactions with dissolved SO_2 may provide significant sinks [*Lind and Kok*, 1986; *Lind et al.*,

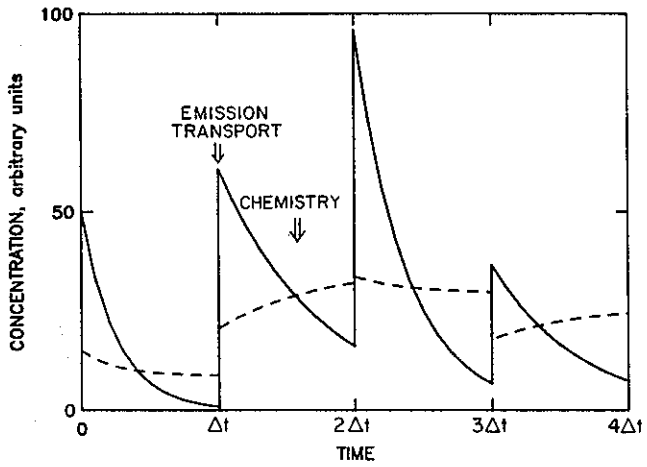

Fig. 1. Application of the CTM operator splitting procedure (equation (1)) to a tracer with short chemical lifetime, showing a hypothetical profile of concentrations versus time for a tracer having a mean chemical lifetime equal to half the CTM time step and no chemical sources. Simulations with no input splitting ($\alpha = 1$; solid line) and with input splitting ($\alpha = 0.3$; dashed line) are compared.

1987], so that a steady state treatment based on gas-phase reactions only would be inadequate. At the levels assumed here, organic peroxides do not contribute significantly to O_3 production in the mechanism of *Lurmann et al.* [1986].

A fixed H_2O_2 concentration of 3 ppb is also assumed. Concentrations measured over North America fall in the range 0-4 ppb [*Heikes et al.*, 1987]; at such concentrations, H_2O_2 has little effect on O_3 production except under very clean conditions. Therefore we do not attempt to simulate H_2O_2 accurately in the CTM, particularly since computation of the source is subject to large uncertainty [*Stockwell*, 1986], and computation of the sink would require estimates of washout and in-cloud reaction with dissolved SO_2.

Reactive nitrogen species are transported as two lumped tracers, NO_x and peroxyacylnitrates (PANs). The concentration of NO_x is defined as the sum of the concentrations of NO, NO_2, NO_3, N_2O_5 (x2), HNO_2, and HNO_4. The individual NO_x species are interconverted rapidly by fast reactions, but the chemical lifetime of the lumped species NO_x is longer, of the order of a few hours. Chemical conversion of NO_x produces HNO_3, PANs, and other organic nitrates. We treat HNO_3 formation as a sink for reactive nitrogen since HNO_3 has a chemical lifetime of several weeks and is removed mainly by deposition. However PANs must be simulated explicitly because they tend to regulate the NO_x concentration in polluted atmospheres, and may provide an important source of NO_x in regions remote from NO_x sources [*Crutzen*, 1979]. We simulate PANs as one lumped chemical tracer composed of fixed proportions of the individual peroxyacylnitrates in the *Lurmann et al.* [1986] mechanism. In the absence of measurements, the proportions are assigned on the basis of photochemical model calculations for typical rural conditions [*Sillman*, 1987].

A significant fraction of total reactive nitrogen may be present as organic nitrates other than PANs [*Fahey et al.*, 1986; *Calvert and Madronich*, 1987]. These organic nitrates may photolyze or react with OH, restoring NO_x. However the rates of reaction are unknown, and there are no concentration data, leaving much uncertainty as to the possible role of organic nitrates in atmospheric chemistry. The *Lurmann et al.* [1986] mechanism assumes that production of organic nitrates is a sink for reactive nitrogen, with the exception of alkylnitrates (Table 2). We have included alkylnitrates as components of the HC1 tracer, consistent with their atmospheric degradation pathways as described by *Lurmann et al.* [1986].

The internal composition of the NO_x tracer is not conserved from time step to time step because it equilibrates rapidly (on a time scale of minutes) with the local environment. The equilibration process produces or consumes O_3, depending on the change in the NO/NO_2 ratio, so that O_3 cannot be used as an independent tracer. We adopt instead odd oxygen (O_x) as the tracer to represent O_3 [cf. *Liu et al.*, 1984]. The concentration of O_x is defined as the sum of the concentrations of O_3, O, NO_2, HNO_4, NO_3 (x2), and N_2O_5 (x3). Interconversion of NO_x species does not affect the concentration of O_x. A consequence of selecting O_x as a tracer instead of O_3 is that the O_3 concentration is not by itself a predicted variable of the CTM. This distinction is unimportant in most of the atmosphere because nitrogen species are negligible contributors to O_x. Only in highly polluted source regions may NO_2 contribute a significant fraction of O_x, and such a condition can be diagnosed in the CTM by comparing the predicted concentrations of NO_x and O_x. Under these polluted conditions the O_3 concentration can be extracted from the CTM output by assuming photochemical steady state between NO, NO_2, and O_3 [*Wu and Niki*, 1975] (at night titration of NO by O_3 or vice versa may be assumed). Ozone concentrations derived from the photochemical steady state assumption must however be interpreted with caution because significant departures from steady state may occur [*Calvert and Stockwell*, 1983].

3. Design of The Chemical Module

The CTM updates the concentration of tracer j, $n_j(x,t)$, over a time step, $[t_0, t_0+\Delta t]$, by successive application of 4 modules describing transport*(T)*, emissions *(E)*, chemistry *(C)*, and deposition *(D)*:

$$n_j(x,t_0+\Delta t) = D \cdot C \cdot E \cdot T \cdot n_j(x,t_0) \qquad (1)$$

The chemical module C must compute the chemical production and loss of tracers over the CTM time step, using as information only the initial tracer concentrations input to the module. We describe here a chemical module (henceforth referred to as the LIV module) which reconstructs the detailed composition of the air parcel from the input tracer concentrations, and integrates the

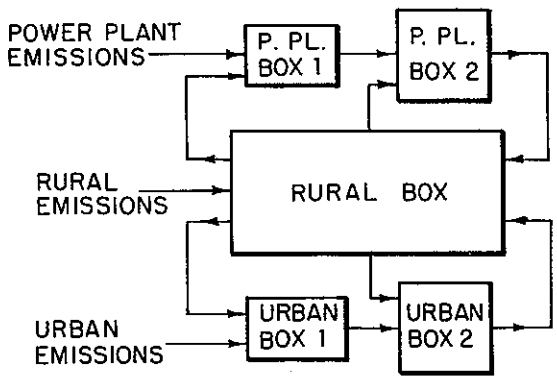

Fig. 2. The Plumes Model: schematic of the subdivision of a CTM grid cell into one rural box, two urban boxes in series, and two power plant boxes in series (Sillman et al., 1989).

TABLE 4. Four-hour Test Simulation: Tracer Concentrations Input to the LIV Module

Tracer	Concentration,[a] ppb
HC1	80
HC2	15
CO	170
NO_x	9.4
PANs	1.6
O_x	32

Meteorological conditions: T = 293 K, P = 950 mbar, relative humidity = 50%. Photolysis rates are calculated for clear summer skies (latitude 40°, solar declination 20°, surface albedo 0.1, O_3 column 300 D.U.) at 1400 LT.

[a] The concentrations of HC1 and HC2 are in units of ppbC. The concentrations of NO_x and HC2 input to the LIV module include contributions from both the initial concentrations at the beginning of the time step and the emissions over the time step.

differential equations representing the detailed mechanism of Lurmann et al. (1986) over the time step $[t_0, t_0+\Delta t]$. For application to the CTM, the production minus loss rates of tracers computed with the LIV module will be fitted to parameterized polynomial functions of the input concentrations of tracers following the procedure described by Spivakovsky et al. (1989).

Proper initialization of the chemical computation is the main difficulty in designing the LIV module. The straightforward approach would be to view the input tracer concentrations as representing initial concentrations at time t_0, but this approach is unsatisfactory for NO_x and HC2 which have chemical lifetimes of the same order as the time step and whose main sources are not chemical but instead fresh emissions or transport from source regions. The concentrations of tracers input to the LIV module include contributions from transport and emissions over the time step $[t_0, t_0+\Delta t]$, as follows from the operator splitting procedure of equation (1). If the concentrations of NO_x and HC2 input to the LIV module were assumed to represent initial concentrations at time t_0 an undesirable "see-saw" profile in the simulated time evolutions of concentrations would result (Figure 1). The concentrations would decrease in a systematic and exaggerated manner over the course of the chemical computation, and jump up after application of emissions and transport. The systematic decreases of NO_x and HC2 concentrations in the chemical computation would lead in turn to bias in the computation of O_3 production. It would be possible to avoid the pulse input from emissions by integrating the tracer emissions into the LIV module, but this procedure would have the undesirable result of increasing the number of independent variables (the tracer emissions would need to be treated as additional independent variables), and thus make eventual parameterization of the module more difficult. Also, even if the pulse from emissions were removed, the operator splitting of chemistry and transport would still produce a see-saw profile.

We try to avoid the systematic decreases of NO_x and HC2 concentrations in the chemical computation by splitting the concentrations input to the LIV module into a fraction α assumed initially present at time t_0, and a fraction $1-\alpha$ emitted (or transported in) at a constant rate over the time step. For the sake of simplicity we

TABLE 5. Results From the Four-hour Test Simulation

	OH 10^6 molecules cm^{-3}	$P-L)_{O_x}$ ppb h^{-1}	$(P-L)_{PANs}$ ppb h^{-1}	$(P-L)_{NO_x}$ ppb h^{-1}
LIV	4.8	10.3	0.76	-1.41
CONTROL	4.9	10.4	0.78	-1.45
Carbonyls x 2	4.2	11.2	1.27	-1.71
Carbonyls / 2	4.7	9.0	0.44	-1.18
		HC1 is 100%		
Propane	5.1	10.3	0.78	-1.45
C_{4-5} alkanes	5.0	9.9	0.71	-1.40
C_{6-8} alkanes	4.0	8.7	0.54	-1.43
C_{4-5} alkylnitrates	4.6	8.4	0.54	-0.93
C_{6-8} alkylnitrates	3.4	8.9	0.53	-0.56
Benzene	5.9	9.2	0.70	-1.38
Toluene	4.9	10.4	1.33	-1.86
Ethylene	4.4	17.1	0.78	-1.35
		HC2 is 100%		
Propene	4.7	9.9	0.70	-1.35
Butene	5.1	11.0	1.21	-1.46
Xylene	5.3	9.8	0.87	-1.55
		PANs is 100%		
PAN	4.9	10.4	0.78	-1.45
Other peroxyacylnitrates	4.8	10.3	0.78	-1.45
$\alpha_{NO_x} = 1$	4.5	9.8	0.67	-1.55
$\alpha_{NO_x} = 0$	4.4	9.3	0.70	-1.24
$\alpha_{HC2} = 1$	4.9	10.7	0.89	-1.54
$\alpha_{HC2} = 0$	4.9	10.1	0.71	-1.40
Input NO_x is 100% NO	4.9	10.4	0.78	-1.45

TABLE 6. Assumed Conditions for the 5-Day Test Simulation

Species	Initial concentration,[a] ppbC	Maximum Emission Rate,[b] ppbC h^{-1}	Deposition Velocity,[c] cm s^{-1}
Propane	9.2	0.125	0
C_{4-5} alkanes	15.0	0.50	0
C_{6-8} alkanes	13.7	1.25	0
C_{4-5} alkylnitrates	0.9	0	0
C_{6-8} alkylnitrates	4.1	0	0
Benzene	3.6	0.025	0
Toluene	4.0	0.5	0
Ethylene	2.0	0.25	0
Isoprene	1.0	2.5[d]	0
Propene	1.5	0.125	0
Butene	0.5	0.125	0
Xylene	1.9	0.125	0
Species	**Initial concentration ppb**	**Maximum Emission Rate,[b] ppb h^{-1}**	**Deposition Velocity,[c] cm s^{-1}**
CO	100	1.25	0
NO	1.0	0.25	0
NO_2	2.0	1.25	1.0
PANs	0.1	0	1.0
O_3	18	0	1.0
carbonyls	steady state	0	0.5

Meteorological conditions: T = 293 K, P = 950 mbar, relative humidity = 50%. Photolysis rates are calculated for clear summer skies (latitude 40°, solar declination 20°, surface albedo 0.1, O_3 column 300 D.U.).

[a] Initial concentrations of hydrocarbons are based on a set of measurements in the Great Smoky Mountains, Tennessee [*Arnts and Meeks*, 1981].

[b] Emission rates are updated every 4 hours by applying a random multiplicative factor between 0 and 1 to the maximum emission rate.

[c] Deposition rates are calculated for a 500 m thick mixed layer. All deposition velocities are halved at night.

[d] Daytime only.

constrain α to be constant over the entire CTM domain (except in subgrid-scale concentrated source regions: see next section). A reasonable criterion for selecting α is that the tracer concentration should remain constant over a time step if the chemical lifetime of the tracer is equal to its mean atmospheric value τ. In this manner the tracer concentration at any time step may either increase or decrease over the course of the chemical computation, depending on the local magnitude of the chemical lifetime relative to τ. Assuming that the tracer has no chemical source, the above criterion leads to the following expression for α:

$$\alpha = (1 + \Delta t/\tau)^{-1} \quad (2)$$

We choose $\alpha = 0.3$ for both NO_x and HC2, since both have mean chemical lifetimes of about 2 hours. Figure 1 illustrates the result of the input splitting procedure with $\alpha = 0.3$. Note that the remaining tracers of Table 1 have either long lifetimes (HC1, CO), or are produced chemically (PANs, O_x); therefore it is not necessary to modify the operator splitting procedure in their cases.

The next task of the LIV module is to decompose the concentrations of the composite tracers into concentrations of the individual species described by the *Lurmann et al.* [1986] mechanism. The procedure is straightforward for HC1, HC2, and PANs, which are decomposed following the mixes of Table 1. To decompose NO_x and O_x we assume that NO, NO_2, and O_3 are the main components of these two tracers, and that their concentrations are related by photochemical steady state (at night we assume that the reaction NO + O_3 goes to completion so that either NO or O_3 is depleted). The chemical computation shows little sensitivity to the assumed speciations of the input NO_x and O_x since interconversion of NO_x and O_x species takes place on a time scale of a few minutes.

After the chemical computation has been initialized and the tracers decomposed into individual species, integration of the photochemical mechanism over the 4-hour time step is routine. We use an implicit finite-difference method [*Richtmeyer*, 1957] with 15-minute increments. The individual species composing the tracers are allowed to evolve independently over the 4-hour time step, so that their relative concentrations may depart from those assumed initially as the tracer composition. For example, over a time step at night the isoprene fraction of HC2 may be depleted but ≈ 70% of the input HC2 will still remain, corresponding to the propene fraction. Under daytime conditions the concentrations of class III hydrocarbons are constrained to remain at steady state throughout the chemical computation, i.e., over each 15-min increment, and the same treatment is applied to short-lived secondary species such as the peroxy radicals. At night the concentrations of

class III hydrocarbons and peroxy radicals are initialized at steady state with an assumed atmospheric composition for the previous afternoon, and are then allowed to evolve as independent variables over the time step. The assumption of daytime steady state for class III hydrocarbons needs to be modified in local source regions (cities, power plants), where concentrations may be systematically below steady state. These modifications are discussed in the next section.

4. Treatment of Urban and Power Plant Plumes

Photochemical calculations with a 4°x5° grid resolution can involve serious errors unless a subgrid structure is used to resolve urban and power plant sources. In our CTM we use the Plumes Model of Sillman et al. (1989) to represent such concentrated source regions. We discuss here the modifications to the LIV module necessary to simulate chemistry in these regions.

A detailed description of the Plumes Model, along with an evaluation of its accuracy, is given by Sillman et al. (1989). The model subdivides each boundary layer CTM grid cell into one rural box, two urban plume boxes in series, and two power plant plume boxes in series (Figure 2). Emissions from cities and power plants are injected into urban box 1 and power plant box 1, respectively. Chemical species in these two polluted boxes are allowed to react in isolation for 4 hours, after which the polluted air is diluted with rural air and transferred to the corresponding box 2, where it ages in isolation for another 4 hours before being ventilated to the rural box.

Application of the LIV module to the rural box of the Plumes Model follows the procedure described in the previous section. Application to the 4 polluted plume boxes requires however changes in two of the assumptions of the LIV module: the steady state assumption for class III hydrocarbons and the splitting of input tracer concentrations between initial concentrations and emissions over the time step. Class III hydrocarbons are not expected to be at steady state in urban box 1 or power plant box 1, due to the large inputs of NO_x and primary hydrocarbons from fresh emissions. Steady state is not expected either in power plant box 2 because of the low reactivity of power plant plumes. In these 3 polluted boxes we initialize the concentrations of class III hydrocarbons at typical rural values and allow these concentrations to evolve as independent variables over the 4-hour time step. The steady state assumption for class III hydrocarbons is retained for urban box 2, since the pollutants input into that box have already aged for 4 hours in the highly reactive environment of urban box 1.

The splitting of input tracer concentrations must be tailored to fit the assumptions defining the polluted boxes of the Plumes Model. Low values of α (0.1) are adopted for NO_x, HC1, and HC2 in urban box 1, in order to simulate the continuous addition of fresh emissions to an initially rural air parcel. Concentrations therefore rise steadily over the 4-hour time step. For urban box 2, the reactivity is controlled mainly by the input of polluted air from urban box 1 at the beginning of the time step, hence $\alpha = 1$ is appropriate for NO_x and HC1; concentrations decrease steadily over the 4-hour time step. The value $\alpha_{HC2} = 0.3$ is retained for urban box 2 in the daytime, since HC2 is contributed mostly by isoprene. We assume $\alpha_{NO_x} = 1$ for both power plant plume boxes since these boxes are specified in the Plumes Model to receive high inputs of NO_x at the beginning of the time step; $\alpha_{HC2} = 0.3$ is retained because power plants are not strong sources of hydrocarbons.

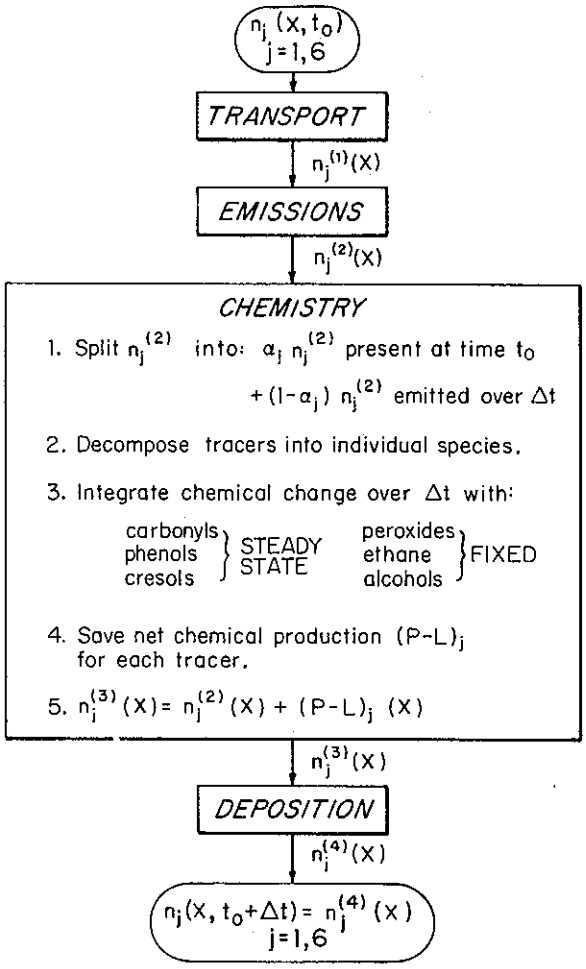

Fig. 3. Schematic of the CTM operator splitting algorithm detailing the simulation of chemistry with the LIV module. The steady state assumptions for carbonyls, phenols, and cresols are modified for nighttime conditions and for simulation of urban and power plant plumes (see text).

5. Accuracy of The Liv Method

The accuracy of the LIV method is evaluated by comparison with detailed model simulations in which all individual species of the *Lurmann et al.* [1986] mechanism are treated as independent variables and are conserved from time step to time step. The tests discussed below focus on simulations of the lower troposphere under conditions of relatively vigorous photochemical activity, when the effects of chemical reactions on tracer concentrations are likely to be most important. The first test examines the sensitivity of the production and loss rates of tracers computed with the LIV module to the individual assumptions invoked by the module. The second test applies the LIV method to simulate the chemical evolution of a stagnant air parcel over 5 diurnal cycles. Finally, the third test applies the LIV method to simulate a sample CTM environment including treatment of polluted source regions with the Plumes Model of Sillman et al. (1989).

5.1. *Test of Individual Assumptions*

The premise of the LIV module is that knowledge of the concentrations of the 6 tracers in Table 1 provides sufficient information to compute the chemical production and loss of these tracers in an air parcel over a 4-hour time step. A number of individual

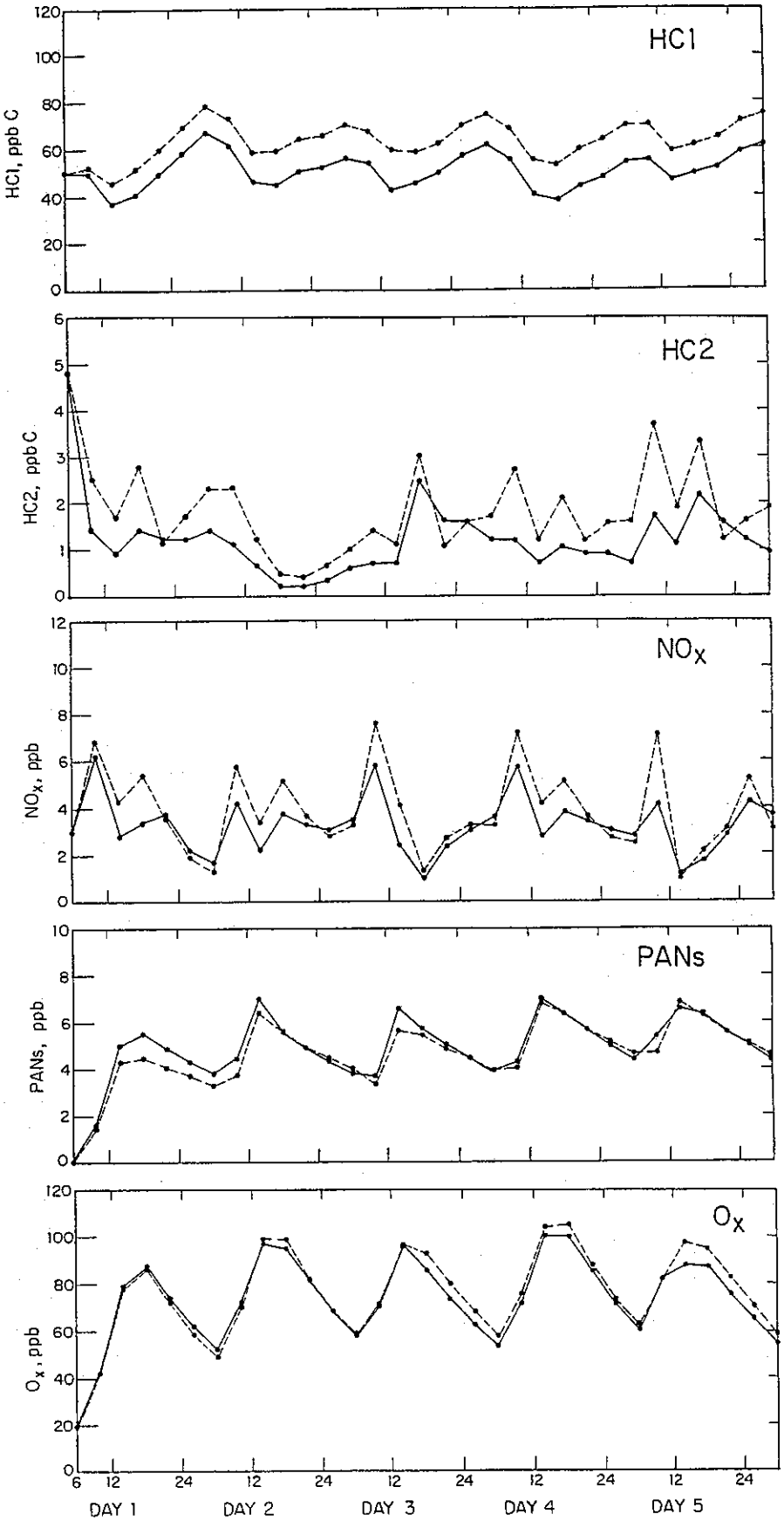

Fig 4. Time evolution of tracer concentrations in the 5-day test simulation. Results from the LIV simulation (solid line) and from the CONTROL simulation (dashed line) are compared.

assumptions are made in defining the initial composition of the air parcel, given the input concentrations of the 6 tracers. Our first test consists of simulating the chemical evolution over 4 hours of a number of air parcels which have different initial compositions but which would all be treated identically in the LIV module because the corresponding input tracer concentrations are identical. The results from these different simulations are compared to the results from the LIV module. The quantities compared are the production minus loss rates of the tracers NO_x, O_x, and PANs, and the 4-hour mean OH concentration (which controls the HC1, HC2, and CO loss rates).

The test is conducted for an air parcel representative of daytime summertime conditions over the rural United States. The air parcel composition is defined in Table 4 in terms of the tracer concentrations input to the LIV module. Application of the LIV module to this air parcel yields the results shown at the top of Table 5. We compare these results to a simulation labeled CONTROL in which the initial composition is made to match exactly that assumed by the LIV module, but in which the concentrations of all species (in particular the class III hydrocarbons) are allowed to evolve independently over the 4-hour time step. As would be expected, the LIV module and the CONTROL simulation are in excellent agreement (see Table 5).

We now conduct a series of 4-hour simulations identical to the CONTROL simulation except that individual features of the initial composition are made to depart substantially from the assumptions of the LIV module. Perturbations are applied to (1) the initial concentrations of class III hydrocarbons, (2) the speciations of HC1, HC2, and PANs, (3) the distributions of NO_x and HC2 between fraction initially present and fraction emitted over the time step, and (4) the speciation of the input NO_x. Results from the different simulations are listed in Table 5. Good agreement is found in most cases with the results of the LIV module; errors are less than 20% in almost all runs. The largest errors are incurred for $(P-L)_{PANs}$, reflecting the sensitivity of PANs production to the concentrations of carbonyl compounds.

Drastic changes in hydrocarbon composition have relatively little effect on the results, as shown in Table 5, unless ethylene or alkylnitrates are dominant contributors to the pool of class I hydrocarbons. If ethylene is dominant then O_x production is seriously underpredicted by the LIV module because ethylene is a stronger source of O_3 and odd hydrogen than other class I hydrocarbons. However, the available concentration data indicate that ethylene is never more than a small fraction of class I hydrocarbons in rural atmospheres. Alkylnitrates decompose to provide a source of NO_x, so that the LIV module overestimates the net loss of NO_x if alkylnitrates dominate class I hydrocarbons (Table 5). This problem cannot be addressed without experimental data on alkylnitrate chemistry and atmospheric concentrations.

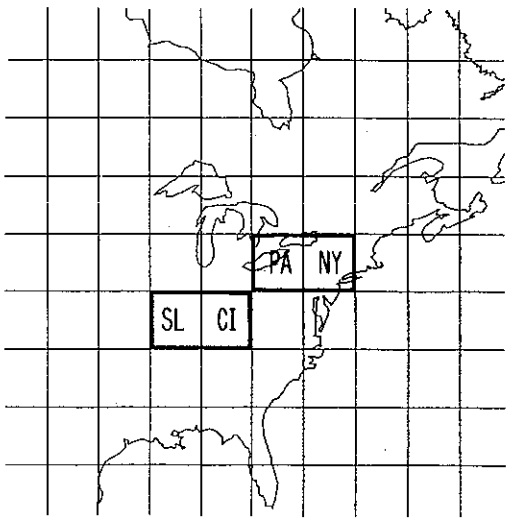

Fig. 5. Detail of the 4°x5° CTM grid over the eastern United States showing the model domains used in the Plumes Model test simulations: Pennsylvania-New York (PANY) and St. Louis-Cincinnati (SLCI).

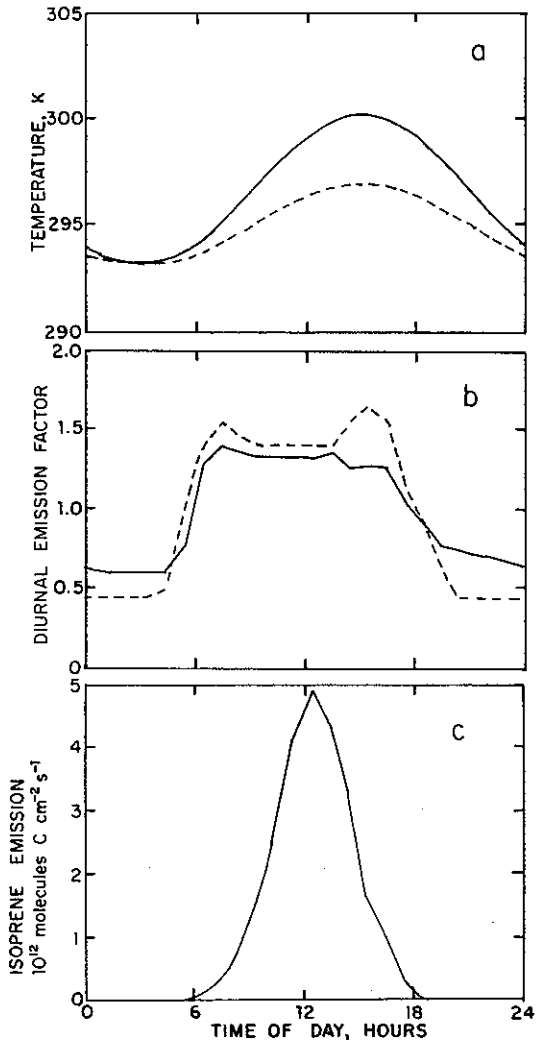

Fig. 6. Diurnal cycles of temperature and emissions in the Plumes Model test simulations. (*a*) Temperature in the PANY simulation (solid line) and in the SLCI simulation (dashed line). (*b*) Multiplicative correction factors to the 24-hour average emission rates of the NAPAP 5.2 inventory, for NO_x (solid line), and for anthropogenic hydrocarbons and CO (dashed line). (*c*) Isoprene emission rates [from *Jacob and Wofsy*, 1988].

5.2. *Simulation over 5 diurnal cycles*

Small errors from the LIV module over a 4-hour time step are unimportant if balanced over subsequent time steps, but could become serious errors if their effects accumulate with time. To examine this possibility we simulate the chemical evolution of a relatively polluted, stagnant mixed layer over 5 diurnal cycles starting from 0600 LT (Table 6). The mixed layer in this simulation is not ventilated in order to amplify the effect of chemistry in con-

TABLE 7. Areas of Plumes Boxes and Tracer Emissions

Plumes Box	Area 10^4 km^2	Emissions,[a] molecules cm^{-2} s^{-1} HC1	HC2[b]	CO	NO_x	O_x[c]
			PA Grid Cell			
Rural	15.2	1.0(12)	1.9(11)	2.8(12)	1.2(11)	1.0(10)
Urban 1	1.08	1.6(13)	2.8(12)	4.2(13)	2.2(12)	1.5(11)
Power Plant 1	0.73	2.1(12)	4.0(11)	4.0(12)	3.2(12)	1.3(11)
Urban 2	1.29	1.0(12)	1.9(11)	2.8(12)	1.2(11)	1.0(10)
Power Plant 2	0.88	1.0(12)	1.9(11)	2.8(12)	1.2(11)	1.0(10)
			NY Grid Cell			
Rural	15.8	1.4(12)	2.3(11)	3.0(12)	1.4(11)	1.2(10)
Urban 1	1.34	2.5(13)	3.7(12)	5.0(13)	2.4(12)	1.7(11)
Power Plant 1	0.13	1.8(12)	3.4(11)	3.5(12)	2.2(12)	7.7(10)
Urban 2	1.73	1.4(12)	2.3(11)	3.0(12)	1.4(11)	1.2(10)
Power Plant 2	0.24	1.4(12)	2.3(11)	3.0(12)	1.4(11)	1.2(10)
			SL Grid Cell			
Rural	14.5	2.8(11)	6.1(10)	5.1(11)	6.3(10)	5.1(9)
Urban 1	0.30	8.6(12)	1.4(12)	2.5(13)	2.2(12)	1.7(11)
Power Plant 1	1.47	4.0(11)	1.2(11)	8.0(11)	3.3(12)	1.0(11)
Urban 2	0.36	2.8(11)	6.1(10)	5.1(11)	6.3(10)	5.1(9)
Power Plant 2	2.60	2.8(11)	6.1(10)	5.1(11)	6.3(10)	5.1(9)
			CI Grid Cell			
Rural	12.8	4.6(11)	7.6(10)	1.0(12)	1.1(11)	9.1(9)
Urban 1	0.69	7.8(12)	1.3(12)	1.7(13)	2.0(12)	1.4(11)
Power Plant 1	1.64	8.1(11)	1.2(11)	1.6(12)	2.9(12)	9.7(10)
Urban 2	0.85	4.6(11)	7.6(10)	1.0(12)	1.1(11)	9.1(9)
Power Plant 2	3.20	4.6(11)	7.6(10)	1.0(12)	1.1(11)	9.1(9)

Read 1.0(12) as 1.0×10^{12}. Emissions are the 24-hour average summer weekday values from the NAPAP 5.2 inventory (in the PANY simulation, hydrocarbon emissions are doubled from the NAPAP values). The diurnal correction factors in Figure 6b are used to calculate emissions at any time of day. Emissions in urban box 2 and power plant box 2 are identical to rural emissions.

[a] Emissions of HC1 and HC2 are in units of molecules C cm^{-2}s^{-1}.

[b] Does not include isoprene emissions, which are taken from Figure 6c.

[c] NO_2 emissions.

trolling tracer concentrations. Deposition is included for some species to maintain their concentrations within reasonable ranges. Emission rates are held at constant values over 4-hour time steps but are arbitrarily changed every 4 hours to a random fraction (different for each individual species) of the maximum values given in Table 6. In this manner the chemical inputs are allowed to change abruptly with time, simulating movement of the air parcel over different source regions.

The LIV simulation follows the concentrations of the 6 tracers in the air parcel using 4-hour time steps and the operator splitting algorithm of equation (1), as illustrated in Figure 3. The concentrations of the 6 tracers are the only quantities conserved from time step to time step. The CONTROL simulation follows independently the time histories of all species in the *Lurmann et al.* [1986] mechanism over the 5-day simulation period, and it integrates emissions and deposition into the chemical computation.

The time evolutions of tracer concentrations in the LIV and CONTROL simulations are compared in Figure 4. Excellent agreement is found for O_x and PANs. Discrepancies of up to 25% are found for HC1 because the mixture of hydrocarbons in the CONTROL simulation is less reactive than that assumed in the HC1 tracer. However the HC1 concentrations do not diverge between the two simulations; the difference remains relatively constant after the first 2 days. The concentrations of NO_x and HC2 are generally in fair agreement, but some discrepancies are apparent, mainly because the splitting of emissions and chemistry within the LIV module does not reflect the actual emission schedule over any particular time step. Since NO_x and HC2 have lifetimes of a few hours, the fine details of their time histories cannot in any case be resolved in a model with operator splitting over a 4-hour time step. The important result is that the conversion rates of NO_x and HC2 are reasonably simulated over an average of time steps, as demonstrated by the good simulations of the secondary tracers O_x and PANs.

5.3. *Two-day simulation with the Plumes Model*

We now apply the LIV method to simulate a model domain consisting of two adjacent grid cells of the 4°x5° CTM grid, with only one layer in the vertical extending from the surface to a fixed upper boundary. Concentrated source regions within the grid cells are resolved with the Plumes Model. Two tests are presented that reproduce the conditions previously used by Sillman et al. (1989) to evaluate the Plumes Model against a 40x40 km^2 Eulerian grid model (*Sillman et al.* 1989, Table 2 (cases B and G)). The Plumes Model simulation as described by Sillman et al. (1989) is used here as the CONTROL simulation.

Two different model domains are investigated (Figure 5): Pennsylvania - New York (PANY), a highly industrialized and populated region, and St. Louis - Cincinnati (SLCI), a less populated

region but with a heavy concentration of power plant NO_x sources. The upper boundaries of the domains are fixed at 700 m in the PANY simulation and 1500 m in the SLCI simulation. No exchange of air is allowed through the upper boundary. A steady westerly wind of 3 m s^{-1} is assumed; such a low wind speed is chosen in order to impose a long residence time for air in a grid cell (46 hours) and thus minimize influences from the boundary conditions (i.e., from air advected into the westerly grid cell).

Both the LIV and CONTROL simulations use 4-hour time steps to simulate transport from Plumes box to Plumes box, and from grid cell to grid cell. The LIV simulation follows the operator splitting procedure illustrated in Figure 3, conserving only the concentrations of the 6 tracers in each box at the end of a 4-hour time step. The CONTROL simulation follows independently the time histories of all species of the *Lurmann et al.* [1986] mechanism, conserving all concentrations from time step to time step and during transport. The CONTROL simulation also integrates emissions and deposition into the chemical computation, thus avoiding the operator splitting of the LIV simulation. Emission rates and meteorological variables (temperature, insolation) are updated every 15 min in the CONTROL simulation, while 4-hour means are used in the LIV simulation.

The air entering the westerly grid cell is assumed to contain background concentrations of O_3 (40 ppb), NO_x (0.26 ppb), hydrocarbons (10 ppbC), CO (200 ppb), and PANs (0.08 ppb).

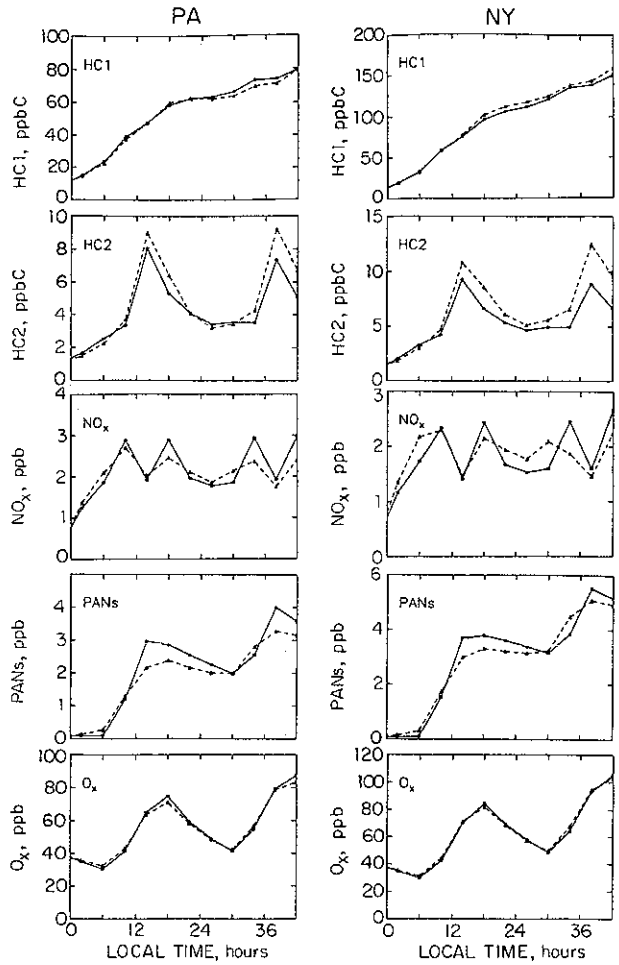

Fig. 7. Time evolution of mean tracer concentrations in the PA and NY grid cells. Results from the LIV simulation (solid lines) and from the CONTROL simulation (dashed lines) are compared.

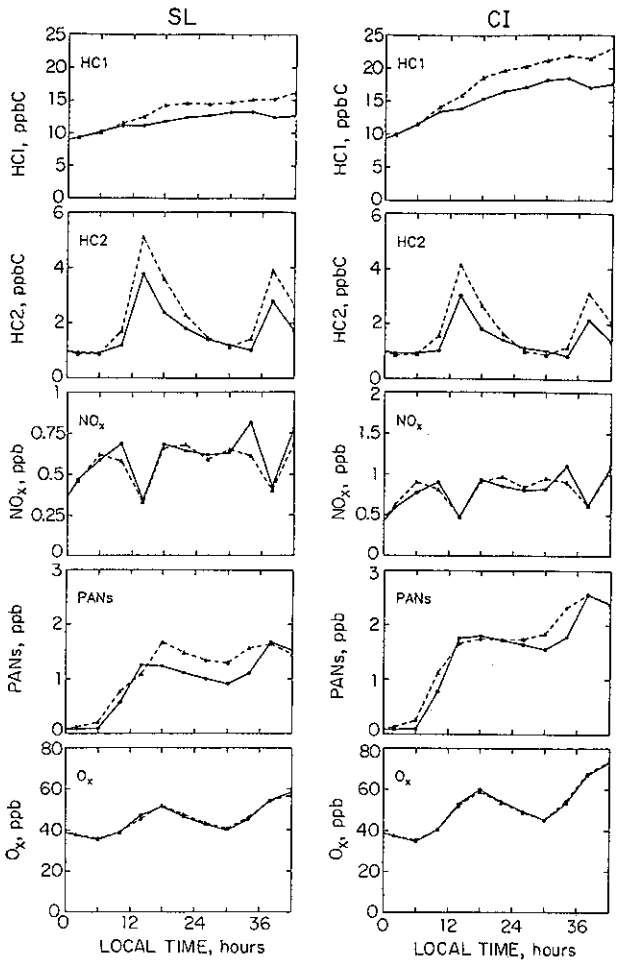

Fig. 8. Time evolution of mean tracer concentrations in the SL and CI grid cells. Results from the LIV simulation (solid lines) and from the CONTROL simulation (dashed lines) are compared.

Deposition velocities are fixed at 0.6 cm s^{-1} for O_3 and NO_2, 0.1 cm s^{-1} for NO, 0.25 cm s^{-1} for PANs, and 1 cm s^{-1} for peroxides (deposition of peroxides is included only in the CONTROL simulation). The simulations are initialized at 2200 LT with the background concentrations. Photolysis rates are calculated for clear summer skies (40°N latitude, 20° solar declination, surface albedo 0.15, O_3 column 310 Dobson Units (DU)). Temperature varies with time of day as shown in Figure 6a.

Emissions of NO_x and anthropogenic hydrocarbons are taken from the NAPAP 5.2 average emissions inventory for a summer weekday [*EPA*, 1986], and are adjusted for diurnal variations as shown in Figure 6b. Emissions of anthropogenic hydrocarbons in the PANY simulation are doubled from the NAPAP values in order to produce highly polluted conditions. Isoprene emissions are assumed to be spatially uniform and vary with time of day as shown in Figure 6c. In the LIV simulation the tracer emissions are computed by lumping emissions of individual species, and averaging these emissions over 4-hour time steps. Table 7 lists the areas of the Plumes boxes and the corresponding emission rates of tracers.

Figures 7 and 8 show the time evolution of mean tracer concentrations in each grid cell computed with the LIV and CONTROL simulations, for the PANY and SLCI tests, respectively. The mean concentration in a grid cell is defined as the area-weighted

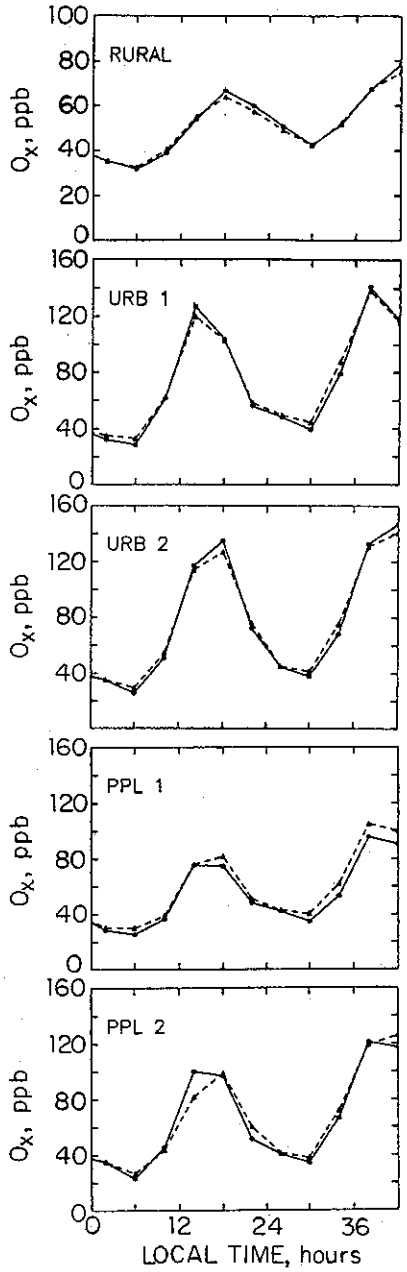

Fig. 9. Time evolution of O_x concentrations in the individual Plumes boxes of the PA grid cell. Results from the LIV simulation (solid lines) and from the CONTROL simulation (dashed lines) are compared.

average concentration from the 5 different Plumes boxes composing the grid cell (Figure 2). Results for CO are not shown since over a 2-day time scale the CO concentrations are controlled primarily by emissions and transport, not chemistry. The results cover a wide range of conditions, from relatively clean (SL) to heavily polluted (NY) (note the differences in scale on the figures). Overall, the agreement between the LIV and CONTROL simulations is very good, under all test conditions. In particular, the agreement is excellent for O_x. Comparison of individual Plumes boxes within grid cells also indicates excellent agreement, as illustrated in Figure 9 for the PA grid cell. These results lend confidence in the ability of the LIV module to predict photochemical production of O_3 over a wide range of NO_x and hydrocarbon concentrations encountered over North America.

Some discrepancies are apparent in Figures 7 and 8 for hydrocarbons, NO_x and PANs, but these never exceed 35%. The discrepancies for NO_x and HC2 originate primarily from the operator splitting procedure, as discussed in section 5.2. In the case of PANs, the discrepancies between the two runs are mostly due to departures of the concentrations of carbonyls from steady state. The concentrations of HC1 predicted by the LIV and CONTROL simulations agree closely in the PANY test, but this agreement is somewhat deceiving because the high HC1 inputs from fresh emissions overwhelm the chemical sink. In the SLCI test, where the effect of the chemical sink is more obvious, the LIV simulation predicts lower concentrations than the CONTROL simulation, because the actual mixture of long-lived hydrocarbons in the SLCI environment is less reactive than that assumed in the LIV simulation. It is inevitable that, depending on the mixture of long-lived hydrocarbons in a particular environment, some error will be made in computing the HC1 lifetime. However this error is relatively small, and not systematic; in particular the error appears to be reversed in the PA grid cell where the LIV mixture is not sufficiently reactive. The LIV mix could possibly be tailored to particular regional mixes but this level of detail is not warranted by the current state of knowledge.

6. CONCLUSIONS

The tropospheric chemistry of O_3, NO_x, and hydrocarbons involves hundreds of species with lifetimes ranging from seconds to weeks. This mix must be treated in a simplified manner in large-scale models of tropospheric O_3. We have designed a least independent variables (LIV) method that reduces the problem to 6 composite tracers, using operator splitting to aggregate rapid chemical transformations into 4-hour time steps. A variety of atmospheric simulations were presented under conditions designed to amplify errors in the LIV method. We found little loss in accuracy compared to detailed model simulations of chemistry with high time resolution. Tropospheric photochemistry can therefore be simulated in a very compact manner, as functions of 6 independent variables. A subsequent paper will show that these functions can be represented as polynomial functions of the concentrations of the 6 tracers, allowing efficient computation of chemical rates in three-dimensional model applications.

Acknowledgements. We thank C. M. Spivakovsky (Harvard University) for helpful discussions. This work was supported by the Coordinating Research Council Grant (Project AP-9), by the National Science Foundation (NSF-ATM84-13153), and by the Environmental Protection Agency (EPA-R814535-01-0).

REFERENCES

Altshuller, A. P., Review: Natural volatile organic substances and their effect on air quality in the United States, *Atmos. Environ.*, *17*, 2131-2165, 1983.

Arnts, R. R., and S. A. Meeks, Biogenic hydrocarbon contribution to the ambient air of selected areas, *Atmos. Environ.*, *15*, 1643-1651, 1981.

Calvert, J. G., and S. Madronich, Theoretical study of the initial products of the atmospheric oxidation of hydrocarbons, *J. Geophys. Res.*, *92*, 2211-2220, 1987.

Calvert, J. G., and W. R. Stockwell, Deviations from the O_3-NO-NO_2 photostationary state in tropospheric chemistry, *Can. J. Chem.*, *61*, 983-992, 1983.

Chameides, W. L., and J. C. G. Walker, A photochemical theory of tropospheric ozone, *J. Geophys. Res.*, *78*, 8751-8760, 1973.

Crutzen, P. J., The role of NO and NO_2 in the chemistry of the troposphere and stratosphere, *Annu. Rev. Earth Planet. Sci.*, *7*, 443-472, 1979.